Journal of Paleolimnology **30:** 343–362, 2003.

A ~33,000 year record of environmental change from Arolik Lake, Ahklun Mountains, Alaska, USA

Darrell S. Kaufman[1,*], Feng Sheng Hu[2], Jason P. Briner[3], Al Werner[4], Bruce P. Finney[5] and Irene Gregory-Eaves[6]

*[1]Department of Geology and Department of Environmental Sciences, Northern Arizona University, Flagstaff, AZ 86011-4099, USA; [2]Departments of Plant Biology and Geology, University of Illinois, Urbana, IL 61801, USA; [3]Institute of Arctic and Alpine Research, University of Colorado, Boulder, CO 83609-0450, USA; [4]Department of Earth and Environment, Mount Holyoke College, South Hadley, MA 01075, USA; [5]Institute of Marine Science, University of Alaska, Fairbanks, AK 99775, USA; [6]Department of Biology, Queen's University, Kingston, Ontario K7L 3N6, Canada; *Author for correspondence (e-mail: Darrell.Kaufman@nau.edu)*

Received 18 December 2002; accepted in revised form 24 March 2003

Key words: Ahklun Mountains, Alaska, Lake core, Paleoenvironment, Quaternary

Abstract

A continuous record of lacustrine sedimentation capturing the entire full-glacial period was obtained from Arolik Lake in the Ahklun Mountains, southwestern Alaska. Fluctuations in magnetic susceptibility (MS), grain size, organic-matter (OM) content, C/N ratios, $\delta^{13}C$, and biogenic silica (BSi) record marked environmental changes within the lake and its watershed during the last ~33 cal ka. Age control is provided by 31 ^{14}C ages on plant macrofossils in four cores between 5.2 and 8.6 m long. Major stratigraphic units are traceable throughout the lake subbottom in acoustical profiles, and provisional ages are derived for six prominent tephra beds, which are correlated among the cores. During the interstadial interval between ~33 and 30 cal ka, OM and BSi contents are relatively high with values similar to those of the Pleistocene–Holocene transition, suggesting a similar level of aquatic productivity. During the glacial interval that followed (~30–15 cal ka), OM and BSi decrease in parallel with declining summer insolation. OM and BSi values remain relatively uniform compared with the higher variability before and after this interval, and they show no major shifts that might correlate with climate fluctuations evidenced by the local moraine record, nor with other global climate changes. The glacial interval includes a clay-rich unit with a depauperate diatom assemblage that records the meltwater spillover of an ice-dammed lake. The meltwater pulse, and therefore the maximum extent of ice attained by a major outlet glacier of the Ahklun Mountain ice cap, lasted from ~24 to 22 cal ka. The Pleistocene–Holocene transition (~15–11 cal ka) exhibits the most prominent shifts in OM and BSi, but rapid and dramatic fluctuations in OM and BSi continue throughout the Holocene, indicating pronounced paleoenvrionmental changes.

Introduction

Understanding arctic climatic history is important because high-latitude areas are particularly sensitive to global climatic changes, and because climatically induced environmental changes there can instigate further changes of global consequence (e.g., Kutzbach et al. (1997), Overpeck et al. (1997)). Within the Arctic, Beringia holds a high potential for obtaining records of climate change that extend beyond the last deglaciation (14 ka). Unlike most other high-latitude areas, many depositional basins in Beringia, including lakes, escaped erosion by late Wisconsin glaciers, and thus preserve an extensive record that captures the inception and full-glacial phases of the last glacial maximum (LGM). Nevertheless, only a few paleoenvironmental records from Beringia that span the LGM have

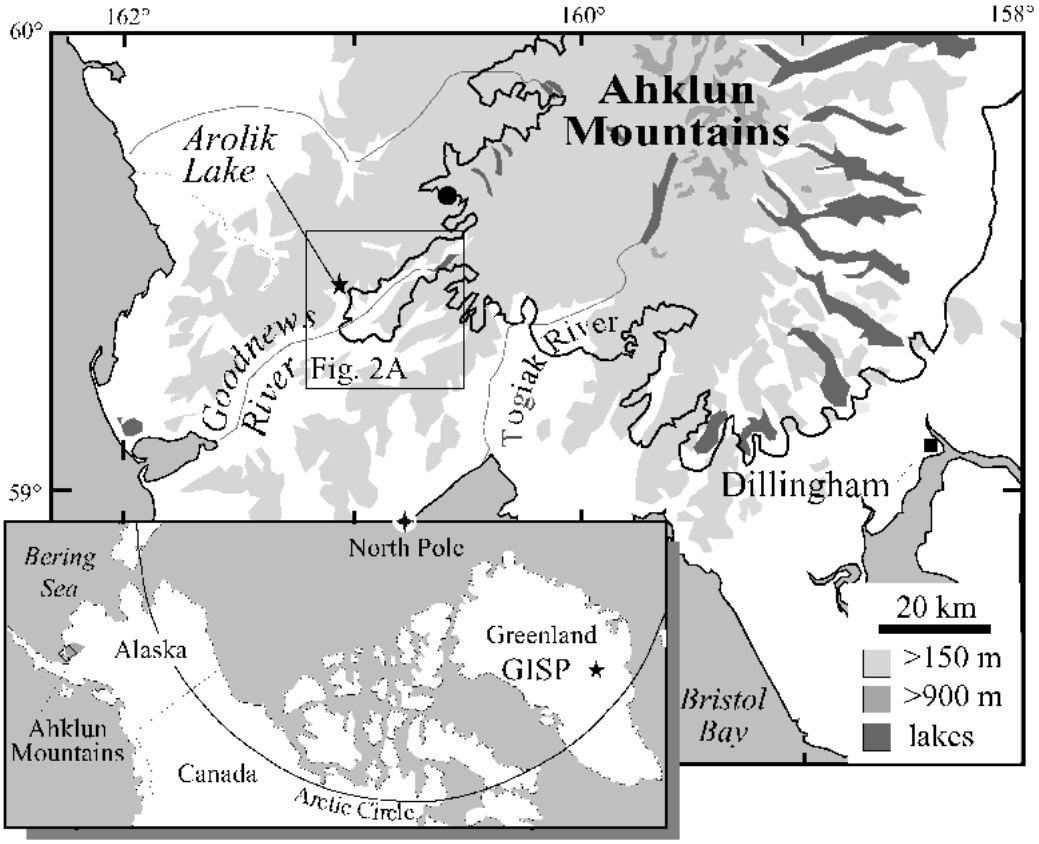

Figure 1. Study area showing extent of the Ahklun Mountains ice cap during the last glacial maximum (solid line) and location of ^{36}Cl-dated moraine (solid circle; Briner et al. (2001)).

yet been recovered (e.g., Anderson and Brubaker (1994)).

The Ahklun Mountains, located in southwestern Alaska, encompass an extensive array of lakes, many situated beyond the limit of late Wisconsin glaciers (Figure 1). Other than the work of Hu et al. (1995, 2002), who studied several lakes within the limit of late Wisconsin ice, no previous research has been published on the paleoenvironmental record from these lakes. This study focuses on Arolik Lake in the southwestern part of the range, where we have studied the glacial-geologic record (Briner 1998; Briner and Kaufman 2000; Briner et al. 2001) and have developed a framework for understanding the major late Quaternary geomorphic changes in the drainage basin. Previous work has shown that glaciers expanded into the drainage of Arolik Lake during the LGM, and that this event may be recognized and dated within the sediment of Arolik Lake.

In this study, we apply a suite of complementary proxy climatic indicators to reconstruct millennial-scale paleoenvironmental changes during the last ~33 ka. We focus on sediment cores from Arolik Lake, where we obtained a continuous record of paleoenvironmental change that extends back through the LGM. Such a record has not yet been obtained from southwestern Alaska, but is important for assessing whether the climatic oscillations known in marine and ice cores from North Atlantic region also affected continental regions of northwestern North America.

Setting

Physiography

The Ahklun Mountains trend about 250 km northeast to southwest in southwestern Alaska (Figure 1). The range reaches its highest elevations in the northeast, where summits exceed 1500 m and shelter dozens of modern-day glaciers. In contrast, the southwestern part of the range is rolling uplands punctuated by a

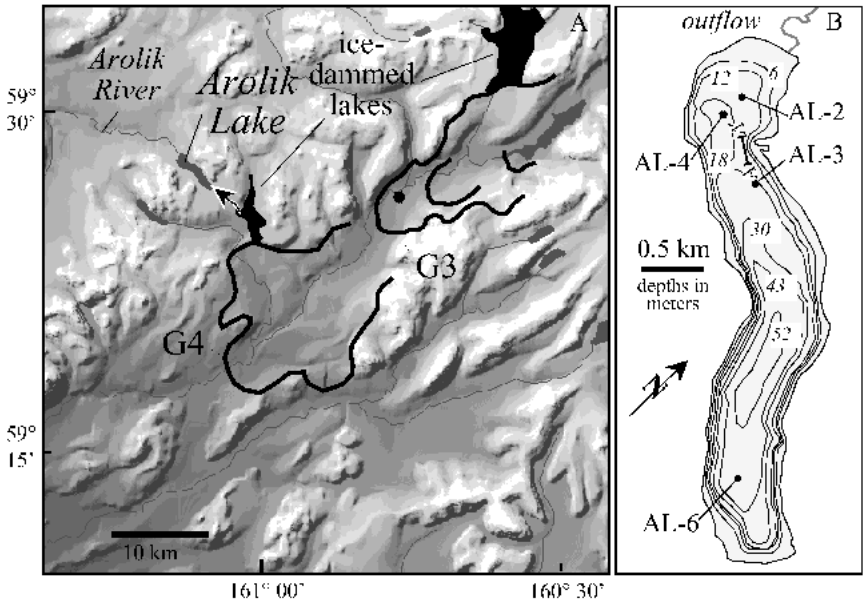

Figure 2. Arolik Lake area showing (A) Goodnews River valley with major end moraines (dark lines), ice-dammed lakes (black), modern lakes (gray), overflow path (arrow), and location of ^{14}C date (solid circle; Manley et al. (2001)); and (B) bathymetry of Arolik Lake with core sites (solid circles) and acoustic-profile transect (Figure 3). See Figure 1 for map location.

few rugged massifs and incised by broad, fault-bounded, river valleys, including the Goodnews and Togiak River valleys.

Arolik Lake (Figure 2) is located along the southwestern flank of the Ahklun Mountains (59° 28′ N, 161° 07′ W), ~100 km northwest of Dillingham on the north side of Bristol Bay. It resides within a trough adjacent to the Goodnews River valley, which was excavated by glaciers into Mesozoic siliciclastic metasedimentary rocks (Hoare and Coonrad 1961). Arolik Lake is 3.7 km long and 0.6 km wide with a surface area of 2.0 km^2, constituting ~20% of the total catchment area. It forms the headwaters of the Arolik River, which flows northwestward to Kuskokwim Bay. The lake surface elevation is 145 m asl. The lake comprises two subbasins: the main subbasin is 53 m deep, forming the elongate axis of the lake; a secondary basin, 18 m deep and separated from the main basin by a minor sill, occupies the outflow (northwestern) end of the lake.

Arolik Lake is within the modern Transitional Zone between maritime and continental climates, and within the zone of discontinuous permafrost (Péwé 1975). Within the region, dwarf scrub communities dominated by ericaceous, birch, and alder shrubs are the primary vegetation cover.

Glacial history

During repeated Pleistocene glaciations, an ice cap developed over the eastern part of the Ahklun Mountains, and alpine glaciers expanded from isolated massifs throughout the western part of the range. Outlet glaciers excavated an extensive network of valley troughs and deposited moraines that confine numerous lake basins, including Arolik Lake. The trough containing Arolik Lake was last occupied by glacier ice during the early Wisconsin, but remained just beyond the limit of glaciers during the LGM (Figure 1).

The 'Arolik Lake glaciation' is named for the moraine that encloses Arolik Lake on its northwestern end (Briner and Kaufman 2000). Cosmogenic exposure dating (Briner et al. 2001) of a nearby, correlative moraine indicates that the advance culminated 60.3±3.2 ka. The Arolik Lake moraine was deposited by a distributary lobe of an outlet glacier that flowed down the Goodnews River valley, the principal ice drainage route for the southwestern sector of the Ahklun Mountains ice cap during Pleistocene glacial phases. During the Arolik Lake glaciation, the Goodnews River valley outlet glacier overtopped low drainage divides along its northwestern margin and splayed northwestward into the Arolik Lake valley and other adjacent troughs.

During the late Wisconsin 'Klak Creek glaciation' thinner and less-extensive ice was constrained within the Goodnews River valley (Briner and Kaufman 2000). Instead of flowing across the low drainage divides along its northwestern margin, the outlet glacier impounded rivers tributary to the Goodnews River, forming an extensive network of ice-marginal lakes. Briner and Kaufman (2000) described one of these lakes, which was dammed by the Goodnews River valley outlet glacier when it reached the position of the G3 moraine (the third major end moraine down the Goodnews River valley mapped by Manley et al. (2001); Figure 2A). On the basis of the mapping and relative-age study of Manley et al. (2001), Briner and Kaufman (2000) attributed the lake and the G3 moraine to the LGM. Our new lake cores and ^{14}C chronology, however, now show that the LGM limit in the Goodnews River is instead represented by the G4 moraine, consistent with some, but not all, of the relative-weathering characteristics of this moraine (Manley et al. 2001).

Methods

The subbottom stratigraphy of Arolik Lake was surveyed using an EdgeTech Geostar acoustic profiling system operating between 4 and 24 kHz. The results guided selection of core sites and allowed correlation of prominent stratigraphic units throughout the lake. Cores were recovered using a percussion corer operated from a floating platform. Four cores, each 7.5 cm in diameter and up to $\sim$8.6 m long, were taken from water depths of up to $\sim$40 m. Two cores (AL-2 and AL-4) were taken from near the center of the northern, secondary basin, distal to the inflow, one core (AL-3) from the slope separating the two main basins, and one (AL-6) from the deep main basin (Figure 2B). The cores were split, photographed, described, and sampled for variety of physical, geochemical, and biological analyses in the laboratory:

(1) Magnetic susceptibility (MS) was measured on all four unsplit cores at 2 cm resolution using a Sapphire Instruments loop detector. Refrigerated cores were brought to room temperature before analysis. Three replicate measurements were averaged to derive the MS at each interval.

(2) Grain size was analyzed using a Coulter LS230 laser diffraction particle-size analyzer. Three of the cores (AL-2, AL-3, and AL-4) were sampled at 5 cm intervals: 0.2–0.4 g of sediment was pretreated by heating in 5 ml of 30% H_2O_2 to remove organics, heated in 10 ml 1 M NaOH to remove diatoms that otherwise would distort the grain-size distribution of the mineral fraction, then shaken in Na hexametaphosphate to disaggregate the sediment for1 h prior to analysis.

(3) Organic-matter and inorganic-carbon content, and bulk density were measured on 1 cm^3 of sediment sampled at 5 cm intervals on all cores. Each sample was dried at 90°C for 6 h, then weighed to measure dry bulk density. Organic-matter (OM) content was approximated by weight loss on ignition (LOI) by combusting samples at 550°C for 2 h. Samples were subsequently heated at 1000°C for 2 h and reweighed to estimate total inorganic carbon (IC) content.

(4) Organic carbon, nitrogen, and $^{13}C/^{12}C$ ratios were analyzed on acid pre-treated samples by a Finnigan Delta Plus mass spectrometer. Isotope results are reported in δ-notation ($\delta = ([R_{sample}/R_{standard}] - 1)*1000$, where $R = {}^{13}C/{}^{12}C$) expressed relative to the international standard Peedee Belemnite (VPDB). Analytical precision for bulk organic $\delta^{13}C$ is better than ±0.1‰.

(5) For biogenic-silica (BSi) analysis, sediment was freeze-dried and ground to powder. BSi was extracted from $\sim$100 mg of sediment with 10% Na_2CO_3 and the concentration determined with a spectrophotometer (Spectronic Genesys5) following the procedure of Mortlock and Froelich (1989).

(6) Diatom assemblages were determined using standard procedures (Battarbee et al. 2001), with400 diatom valves identified and enumerated for each sample.

(7) Thirty-nine radiocarbon (^{14}C) ages were obtained from the four cores, plus one from a living aquatic plant. Most of the samples (31), including all 23 from AL-4, comprised macrofossils derived from sediment intervals typically 2 cm thick (Table 1). Macrofossils were hand-picked from the150 μm fraction; they included a mixture of detrital wood, seeds, insects, and mosses, although some were composed entirely of wood. Core AL-4 yielded the most macrofossils. Because macrofossils were sparse in other cores, we dated organic fractions derived from bulk sediment, including six humic acid and two humin extracts, all processed at the University of Colorado's INSTAAR Laboratory. In addition, three samples were prepared using a standard pollen preparation procedure (Faegri et al. 1992) to yield a concentration of finely disseminated pollen, charcoal, and uni-

Table 1. AMS ^{14}C ages, Arolik Lake.

Depth (cm)	Sample type*	^{14}C age (yr BP)	Calibrated age (cal yr BP)†	Lab-ID (NRSL)
Lake surface	aquatic plant	1.0763±0.0043 (fraction modern)		10541
Core AL-4				
3–5	mixed macrofossils	2390±65	2525±180	11363
11	wood	2590±85	2660±115	11364
64–66	wood	2800±45	2900±50	11365
111–112	leaves+other macros	5295±30	6080±90	86531††
136–138	mixed macrofossils	6150±55	7060±115	11366
158–159	moss	7515±35	8295±75	86532††
182	wood	8310±65	9310±160	11367
200–201	wood	8905±35	10,040±125	86533††
246–248	mixed macrofossils	9960±95	11,395±165	11368
253–255	wood (small sample)	10,550±230	12,505±395	79689††
277–278	single twig	11,850±40	13,845±185	79690††
319–321	mixed macrofossils	10,970±75	13,010±120	11369
330–333	moss (small sample)	7160±210	7965±210	81525††
362–363	large wood	13875±50	16650±235	81526††
362–364	moss	13,650±110	16,390±260	81527††
366–368	mixed macrofossils	9880±55	11,250±50	11544
392–393	mixed macrofossils	12,490±80	14,855±565	81528††
422–424	mixed macrofossils	13,190±65	15,860±230	11545
480–482	mixed macrofossils	15,890±75	18,975±305	11546
691–693	mixed macrofossils	20,530±130	24,000±1000	11370
745–749	mixed macrofossils	24,800±140	28,000±1000	11547
798–800	mixed macrofossils	28,500±220	32,000±1000	11371
849–851	mixed macrofossils	30,730±260	33,000±1000	11372
Core AL-3				
49	wood	6180±45	7100±100	10542
88	wood	8850±55	9970±180	10543
90–91	humins	9700±95	11,010±190	10938
139–141	mixed macrofossils	10,700±60	12,780±140	10544
181–183	mixed macrofossils	8130±80	9130±120	11542
202–203	humic acids	14,600±85	17,490±270	10545
207–209	mixed macrofossils	11,250±60	13,250±110	11543
279	wood	16,500±85	19,670±320	10546
350–351	humic acids	25,700±210	28,000±1000	10547
397–398	humic acids	24,900±200	27,000±1000	10548
530–531	humic acids	28,900±280	32,000±1000	10549
616–617	humic acids	29,800±450	33,000±1000	10550
617–619	mixed macrofossils	22,150±230	25,000±1000	26592**
620–621	humin	34,300±410	35,000±1000	10939
692–693	humic acids	32,700±600	35,000±1000	10551
Core AL-2				
203–204	pollen concentrate	20,500±150	24,000±1000	11073
400–403	pollen concentrate	2,5900±140	28,000±1000	11061
507–508	pollen concentrate	16,050±95	19,160±320	11062
Core AL-6				
558	wood	12,440±65	14,820±570	11548

*Mixed macrofossils=various proportions of mosses, sedges, and seeds, leaves, wood frags, and insects; pollen concentrate=finely disseminated pollen, charcoal, and unidentified humified organic matter.

†Calibrated ages according to Stuiver et al. (1998) presented as the midpoint±one-half of the 1σ range; ages older than 20 ^{14}C ka were calibrated using a graphical interpretation of Figure 1A in Kitagawa and van der Plicht (1998) and an assumed uncertainty of ±1000 yr.

**NSF-University of Arizona Laboratory (AA).

††Lawrence Livermore National Laboratory, Center for Accelerator Mass Spectrometry (CAMS).

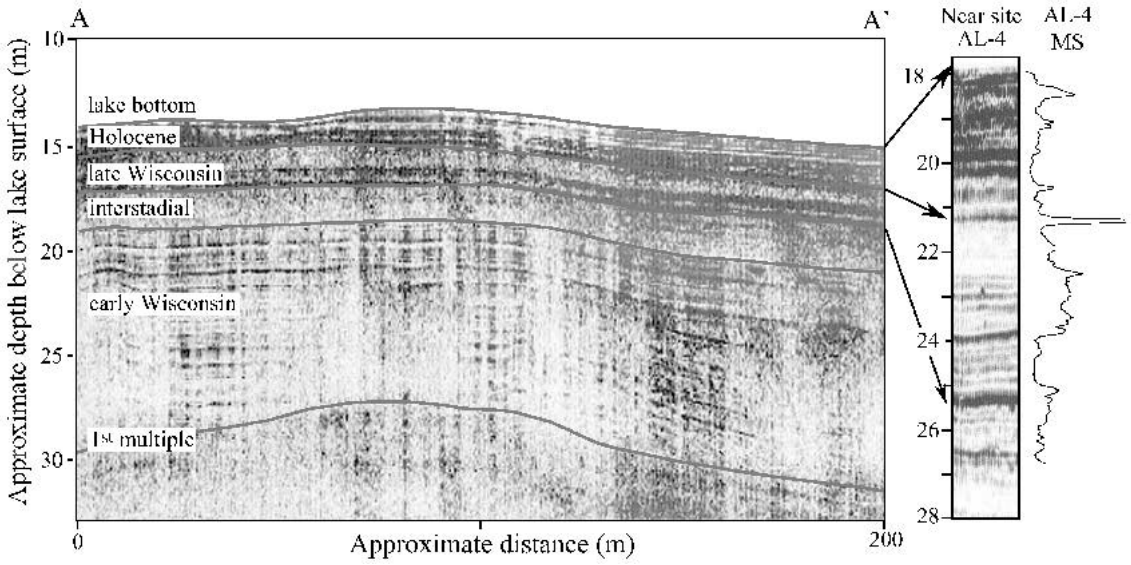

Figure 3. Arolik Lake subbottom acoustic stratigraphy. Main panel shows transect A–A′ (Figure 2B); panel on right is from near core site AL-4. The 8.6-m-long magnetic susceptibility (MS) record from core AL-4 (Figure 4) is plotted along side the acoustic profile. Note the thicker acoustic-stratigraphic units at the core site; correlations between major units shown by dotted lines with arrows. Depth scale for both profiles is inferred using a travel velocity of 5000 ft s^{-1}.

dentified humified organic matter. ^{14}C ages <20 ka were calibrated using the mid-point±one half of the 1σ range of all calibrated-year intercepts specified by CALIB (Stuiver et al. 1998). Calibrated-year ages for samples20 ka were estimated graphically using the U/Th calibration of Kitagawa and van der Plicht (1998). All ages are reported in calibrated years.

Results

Litho- and acoustic stratigraphy

Numerous subbottom acoustic images indicate a total sediment thickness in Arolik Lake of20 m in the deepest basin. The profiles show a consistent succession of sub-parallel acoustic stratigraphic units with no evidence for mass movements. Five units were identified (Figure 3); they thicken in the basins and thin over the sills and toward the lake margins. (1) The oldest strata observed consist of well-layered acoustic reflectors, up to 9 m thick, that were not penetrated by our cores. (2) The basal unit is overlain by a 2- to 5-m-thick homogenous interval, the top of which was recovered at the base of the longest cores. (3) The homogenous interval is followed by 1–2 m of acoustically layered strata that we correlate with the clay-rich unit penetrated by three cores (see below). (4) Overlaying the acoustically layered unit is at least 2 m, and, in places, as much as 5 m of acoustically homogenous strata capped by (5) a 2- to 3-m-thick unit that exhibits strong acoustic reflectors related to Holocene tephra beds near the top of the cores.

Three core sites were selected to sample a range of sedimentation rates. Core AL-6 was from the main, proximal basin, where thickening of seismic reflectors indicates that sedimentation rates are highest. Core AL-3 was from the sill separating the proximal and distal basins, where sedimentation rates are lowest. Cores AL-2 and AL-4 were from the secondary, distal basin, with intermediate sedimentation rates. These two cores also contained the highest concentration of vegetation macrofossils. Core AL-4 received the most attention analytically. Results from the other cores are presented to demonstrate the consistency and integrity of the stratigraphic record.

Sediment recovered in the four cores is dominated by silty mud varying from weakly to strongly laminated (0.2- to 0.5-cm-thick laminations) (Figure 4). Laminations are defined by slight variations in particle size and by variations in color. The cores contain interbeds of mud and detrital organic material and at least six prominent tephra layers. The tephras appear as distinct beds of angular, very fine to medium sand-sized pumice grains, glass shards, and primary minerals. A distinctive ~1-m-thick unit of

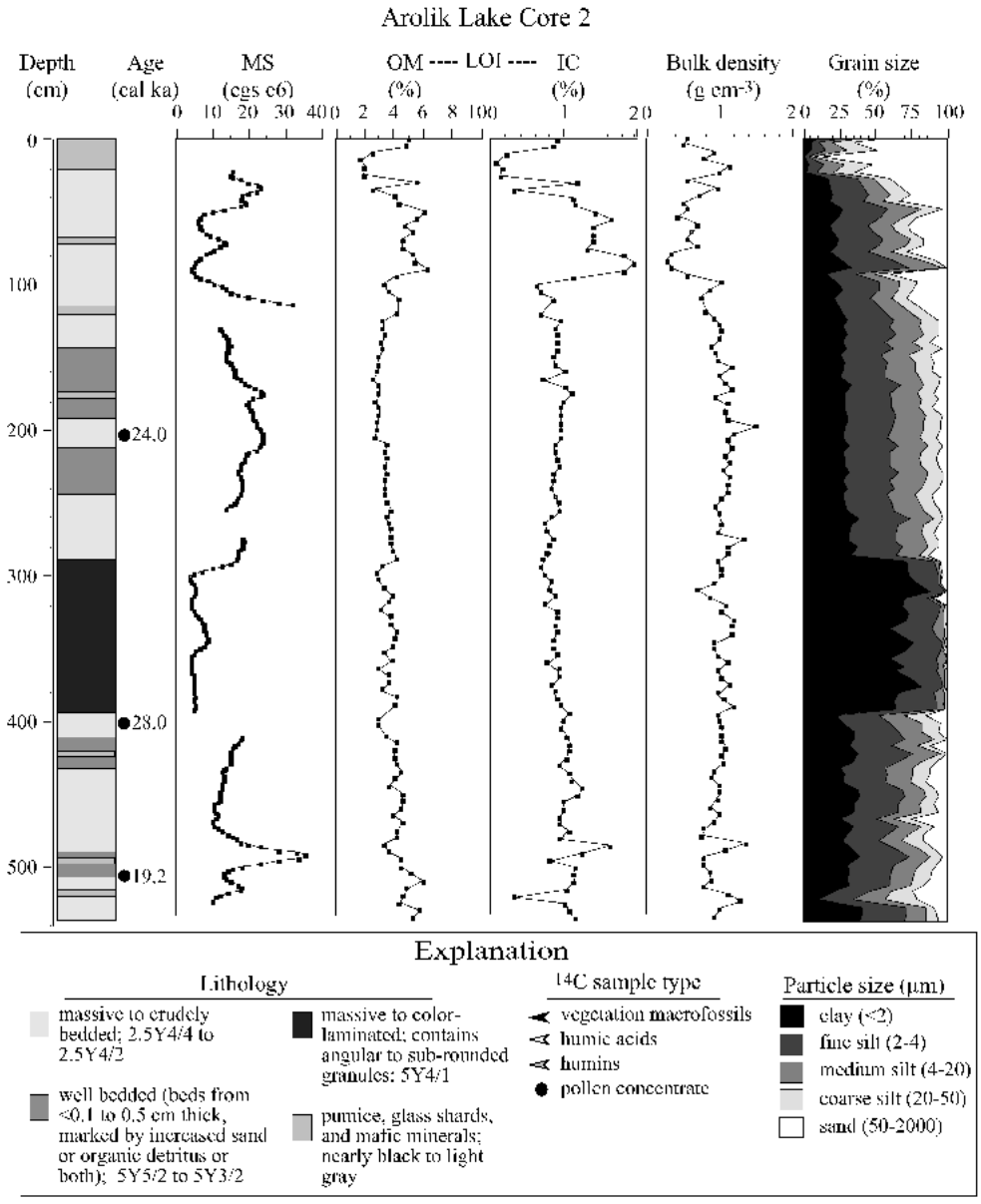

Figure 4. Lithostratigraphy, ^{14}C ages, and magnetic susceptibility (MS), organic-matter (OM) and inorganic-carbon (IC) (based on loss on ignition (LOI)), and bulk density for all cores, particle-size distribution for cores AL-2, AL-3, and AL-4, and biogenic silica (BSi) for core AL-4.

weakly bedded clay (~50% clay and ~20% fine silt) containing angular granules (and one large pebble) is found in the three longest cores. The clay-rich unit is traceable throughout the lake in the acoustic stratigraphy.

^{14}C chronology

On the basis of ^{14}C dating and stratigraphic correlations, three of the four cores (AL-2, AL-3, and AL-4) penetrated sediments ~30 ka or older. Of these three cores, the chronology from AL-4 is based on more macrofossil samples than other cores (Figure 5; Table 1); we therefore focus our discussion and conclusions on this core. Of the 23 ^{14}C ages from core AL-4,

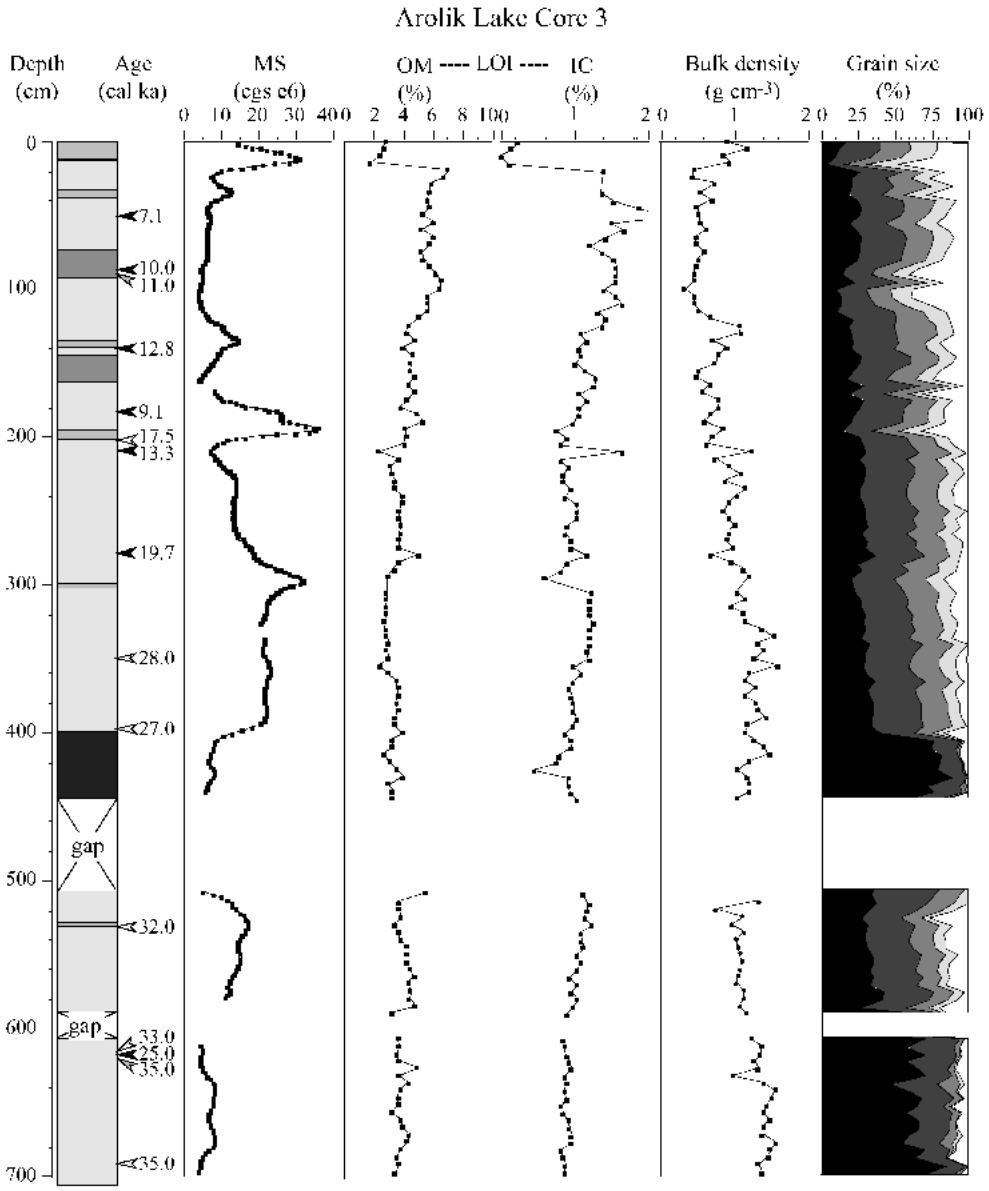

Figure 4. Continued.

six were rejected because they fall off the uniform trend defined by the other ages. The rejected ages are younger than expected, probably due to contamination by an unknown source and because some were too small for an accurate analysis (cf. Oswald et al. (2002)). We rejected the younger ages because they result in tephras ages that are too young compared with correlative tephras in core AL-3 (see below) and in a core taken from Nimgun Lake, 24 km northeast of Arolik Lake (DSK, unpublished data). One of the rejected ages was taken from 10 cm below a prominent, 25-cm-thick tephra bed that we provisionally correlate with the major, well-dated eruption of Aniakchak Volcano at 3.6 ka (Waythomas and Neal 1998), suggesting that the associated ^{14}C age is at least 700 yr too young.

We attribute the $\sim$2 ka age at the top of core AL-4 to losing the upper few decimeters of the core top (common with percussion coring equipment), rather than to a hardwater effect. The absence of carbon-rich lithologies in the drainage indicates that a hardwater effect is unlikely. A date on a single fragment of wood

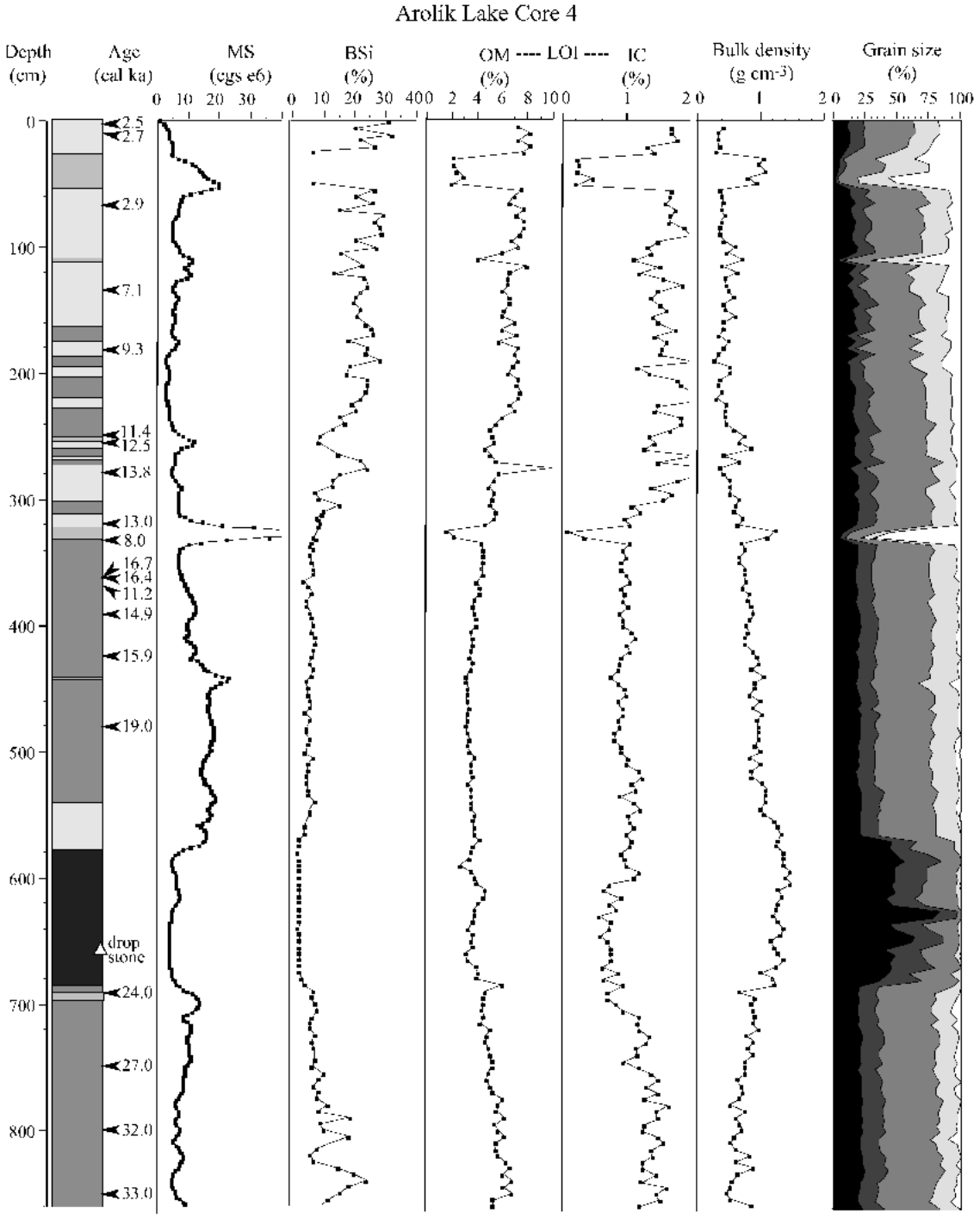

Figure 4. Continued.

from 362 to 363 cm depth overlaps with a date on a mix of macrofossils, including aquatic material, from the same level (Table 1). In addition, living aquatic plants dredged from Arolik Lake yielded ^{14}C activity of the post-bomb era (Table 1), further indicating the lack of a significant hardwater effect.

To derive an age model for AL-4, we subdivided the core into three intervals and fit separate trend lines

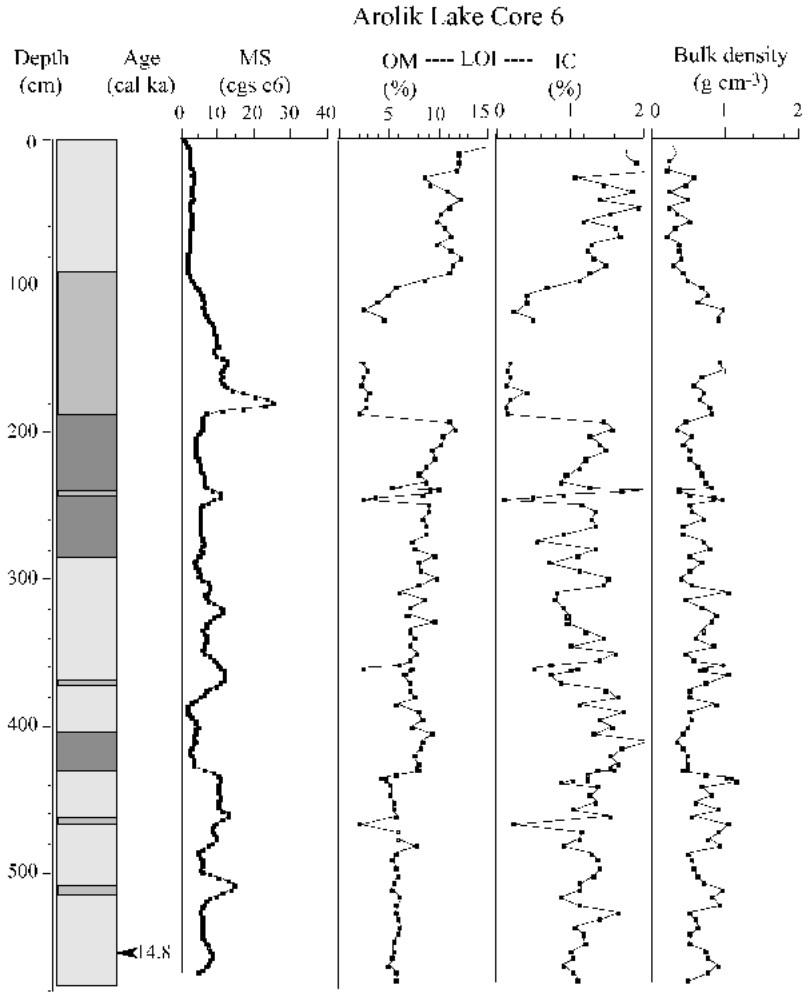

Figure 4. Continued.

to each (Figure 5). The four ^{14}C ages from the lowest segment were fit with a second-order polynomial (R^2=0.991), indicating decreasing sedimentation rates upward through this interval. The middle segment, including twelve ^{14}C ages and one correlated tephra age, was also fit with a second-order polynomial (R^2=0.994). This segment was extrapolated downward through the clay-rich layer, where the trend line meets the top of the lower segment, and was extended upward to the base of the 3.6±0.1 ka Aniakchak (?) tephra at 55 cm. The upper segment extends from the top of the tephra (27 cm), assumed to have been deposited instantaneously, through two additional ^{14}C ages, and was fit with a linear trend (R^2=0.980). The average sedimentation rate in AL-4 is 0.27 mm yr^{-1}. Despite the relatively good fit of the model to the data, we recognize that each calibrated ^{14}C age has an associated error of ±100–300 yr (more for ages20 ka), and therefore, our modeled ages have uncertainties of at least a few hundred years.

Core AL-3 yielded macrofossils for seven ^{14}C ages (Table 1). The ages were fit with a power function (R^2=0.967) after excluding one aberrant result (Figure 5). The overall sedimentation rate is similar to that of nearby core AL-4, and the rate apparently decreases upward. The accuracy of the macrofossil ages is supported by tephrostratigraphic correlations with core AL-4 (see below). Ages on macrofossils are consistently younger than the ages on humic and humin extracts. The difference in age between macrofossils and the organic extracts increases systematically with age. At ~90 cm depth, macrofossils date to ~10 ka, whereas the age on the humin fraction is ~1000 yr older. At 620 cm depth, macrofossils date to ~25 ka,

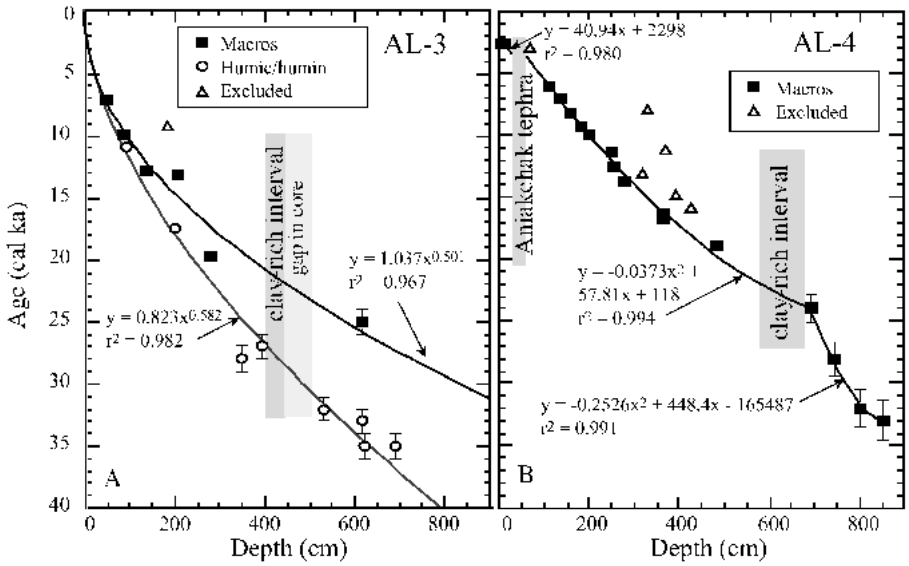

Figure 5. Age models for cores (A) AL-3 and (B) AL-4. Models discussed in text. Ages are midpoints ± one half of 1σ ranges (error bars) for the calibrated ages (data listed in Table 1). Ages shown as open symbols were excluded from calculations.

$\sim$10,000 yr younger than the humic acid fraction from the same sediment. Elsewhere in the Arctic, ages of macrofossils are younger than those of bulk sediment and organic extracts from lake sediment (e.g., Abbott and Stafford (1996) and Miller et al. (1999)). Our data show further evidence of potential errors associated with ages on these organic fractions.

No age model was derived for core AL-2 because the core lacked dateable quantities of macrofossils. By comparison with AL-4, this core probably penetrated sediment as old as $\sim$40 ka. Our attempt to date concentrated disseminated organic matter from pollen preparations on core AL-2 was unsuccessful. Although we cannot compare these pollen-preparation ages with macrofossils ages, the lowest sample (507 cm) yielded the youngest of the three ages, whereas stratigraphic correlation with AL-4 indicates that the other two ages are unexpectedly old.

Magnetic susceptibility and tephra correlations

Magnetic susceptibility (MS) provides a non-destructive, quantitative measure reflecting a combination of sediment properties (density, mineralogy, organic content; e.g., Thompson and Oldfield (1986)). We use MS to correlate cores within and among lakes. MS profiles exhibit major fluctuations in all cores (Figure 4). Prominent peaks in MS coincide with tephra layers. A systematic analysis of the tephras has not been completed, but inspection under binocular microscope indicates that MS is related to proportion of mafic minerals, and the abundance of microlitic glass. MS is moderately high through the prominent tephra near the top of the core (Aniakchak ?). The highest values are associated with the $\sim$15.1 ka, mafic, $\sim$5-cm-thick, sandy tephra, although MS values are somewhat lower for the correlative unit in AL-6. The lowest MS was consistently measured in the clay-rich intervals of each core, suggesting a change in source material, or a dilution effect.

The tephra beds and their associated MS spikes form prominent markers that can be used to correlate among the four cores (Figure 6), and further support the stratigraphic consistency of the sedimentary sequence across the lake. The correlations show systematic differences in the sedimentation rates among the core sites, consistent with their ^{14}C chronologies. The modeled ages of the six correlated tephra beds and the top of the clay-rich unit differ by an average of 2% between cores AL-3 and AL-4 (Table 2). The slightly younger ages in AL-3 might be attributed to the less-accurate ^{14}C age model for that core. Regardless, the overall similarity in tephra-correlated ages lends confidence to the integrity of the chronological control.

Grain size and bulk density

Grain-size changes in Arolik Lake probably reflect changes in provenance of sediment sources (e.g., an influx of tephra or an inflow of glacial meltwater), the

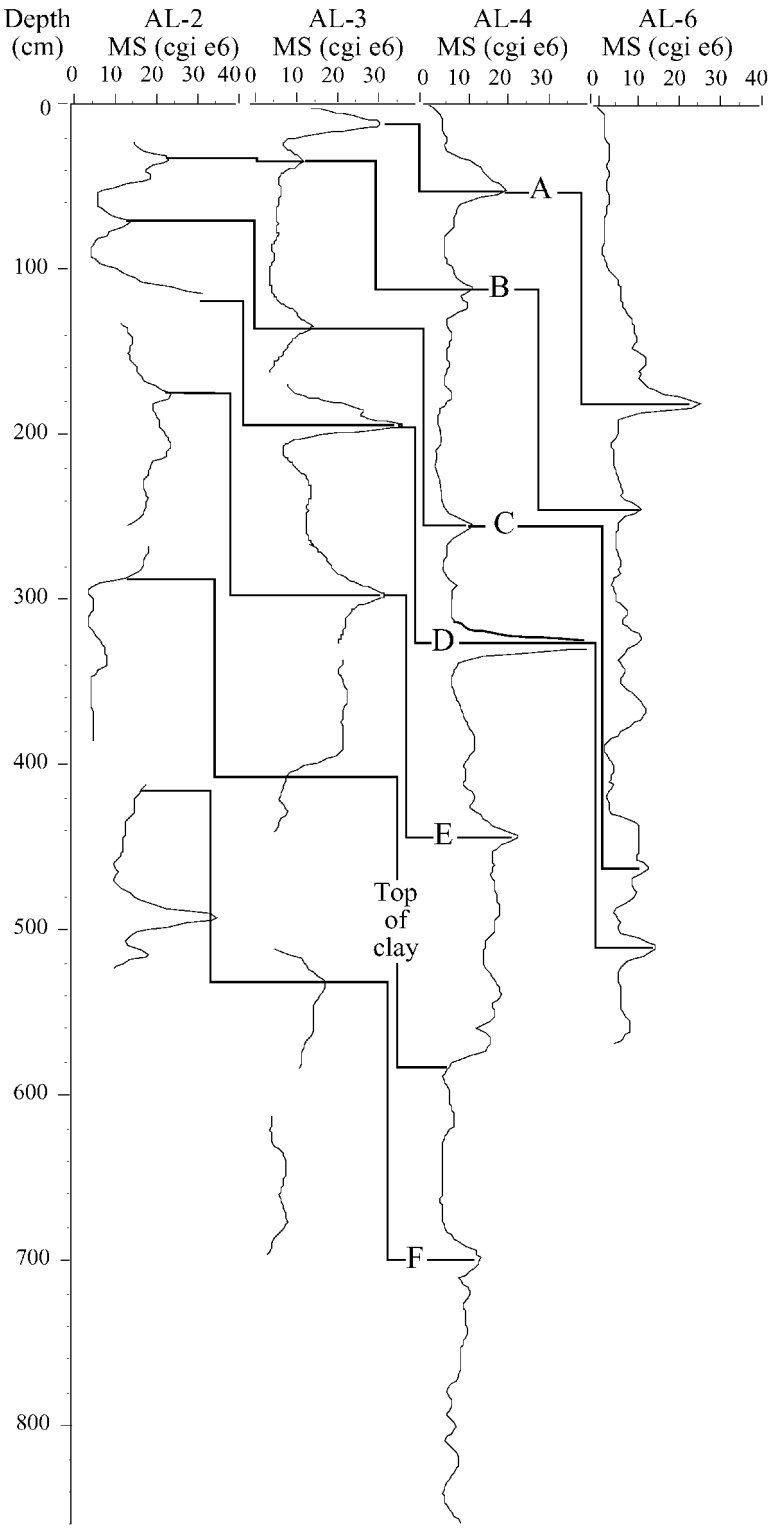

Figure 6. Correlations among cores based on magnetic susceptibility (MS) profiles. Major MS peaks coincide with mafic- and microlite-rich tephra layers of unknown sources.

Table 2. Prominent stratigraphic markers and their modeled ages, Arolik Lake cores AL-3 and AL-4.

Marker	AL-3		AL-4	
	Depth (cm)	Age (ka)	Depth (cm)	Age (ka)
Tephra A	10	3.3	55	3.4
Tephra B	35	6.1	110	6.1
Tephra C	135	12.1	255	12.4
Tephra D	200	14.7	330	15.1
Tephra E	300	18.1	440	18.6
Top of clay	400	20.9	570	21.8
Tephra F	530	24.0	700	24.6

proximity of the sediment source to the core site (e.g., migration of inflow channel, or the dynamics of the depositional environment (e.g., lake-level fluctuations)). Overall, sediment grain size in Arolik Lake is dominated by medium silt (Figure 4). The most prominent shift in grain size is the ~1-m-thick, clay-rich interval in the three oldest cores. Percent clay doubles between consecutive samples across the lower boundary of this interval, and is reduced by one half across the upper contact; coarse silt and sand are nearly absent. Other abrupt changes in grain size are associated with tephra beds. These typically contain a higher proportion of sand grains, although some are finer and not all tephra layers are represented by the 5-cm-sample interval. In addition to these abrupt changes, all cores exhibit a gradual upward coarsening of grain size. In core AL-4, the proportion of grains4 μm (medium silt and coarser) increases from ~60% in the bottom ~1.5 m to ~75% in the upper 2.5 m, while fine silt and clay decrease by ~15% from bottom to top.

Down-core changes in bulk density reflect changes in sedimentology and compaction. Dry sediment bulk density ranges from 0.3 to 1.5 g cm^{-3} and averages ~0.8 g cm^{-3} (Figure 4). Values generally increase with depth, although the clay-rich interval, and some tephra, exhibit the highest bulk densities.

Loss on ignition (inorganic carbon and organic matter)

Changes in inorganic carbon (IC) content reflect changes in sediment sources and possibly endogenic production. IC content is low in Arolik Lake sediment, averaging ~1.2% (Figure 4). Holocene sediment contains a slightly higher proportion of IC compared to Pleistocene sediment, but is too low to draw paleoenvironmental inferences.

Organic-matter (OM) content reflects a number of factors, including aquatic productivity, input of detritus from terrestrial vegetation, and the flux of mineral matter to the lake (e.g., Engstrom and Wright (1984) and Meyers and Ishiwatari (1993)). OM content ranges from 2 to 10% in Arolik Lake sediment (Figure 4). Overall, OM varies slightly among the cores and is highest (average=5%) in AL-4. Tephra layers contain the least OM; Holocene sediment contains the most (6–7%), with a relatively rapid increase near the Pleistocene–Holocene transition. In cores AL-3 and AL-4, OM content is lowest (~3%) in the interval between the base of the clay-rich interval upward to tephra E, dated at ~18.6 ka in AL-4. The interval below the clay-rich unit exhibits an intermediate amount of OM (4–5%). In core AL-2, however, most of the sediment below the clay-rich interval contains little OM (3–4%). Only the lowest 50 cm of this core attains OM values comparable to the Holocene sediment.

Biogenic silica

Biogenic silica (BSi) content is a measure of the abundance of diatoms preserved in lake sediment, which are commonly the main primary producers in lakes (Wetzel 1983). Down-core variation in BSi reflects a number of factors, including physical and chemical properties of the water column, nutrient and light availability, as well as dilution by organic and mineral matter (e.g., Colman et al. (1995)). In AL-4, the only core analyzed, BSi content is relatively high (~5–21%) (Figures 4 and 7). It decreases from 33 to 24 ka, and shows several fluctuations during the early portion of this period. BSi is uniformly low (~2.5%) in the clay-rich unit between 24 and 22 ka. It then increases to 5% by 21.0 ka, followed by a more gradual increase to ~10% by 15.0 ka. During the last glacial-interglacial transition (15–10 ka), BSi fluctuations are most pronounced. During the Holocene, it is consistently high (17% with the exception of two samples) and is marked by continued fluctuations.

Carbon and nitrogen

The elemental and isotopic composition of organic matter is useful in distinguishing aquatic from terrestrial sources (e.g., Meyers and Ishiwatari (1993)). The C/N of AL-4 samples (the only core analyzed) ranges

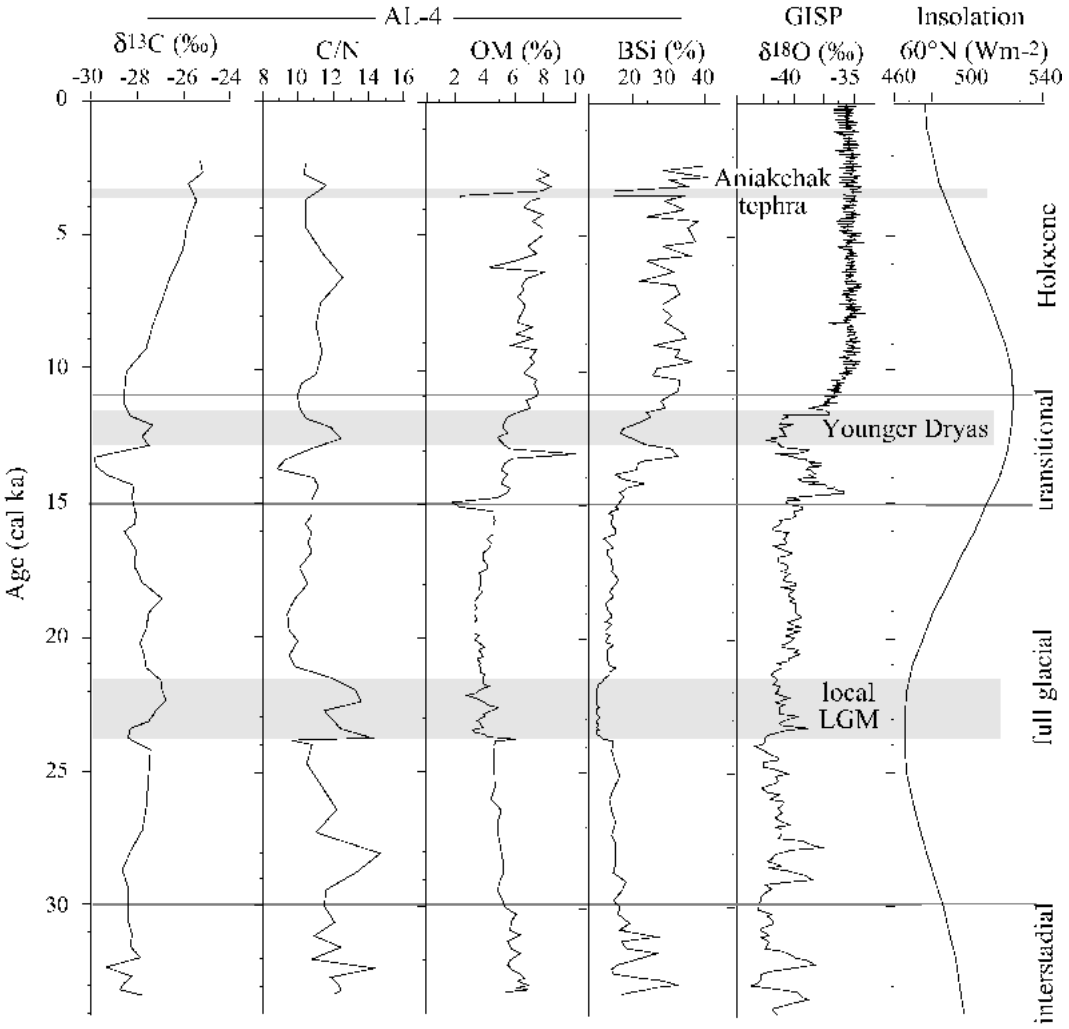

Figure 7. Comparison between proxy environmental indicators in Arolik Lake sediment compared with $\delta^{18}O$ of Greenland ice and June insolation for the last 34 ka. Paleoproductivity indices from AL-4 include: $\delta^{13}C$ and C/N composition of organic matter, and the weight percent of organic matter (OM) and biogenic silica (BSi) content. Time scale for AL-4 is based on age model shown in Figure 5B. Time scale for the Greenland ice core (GISP) from Meese et al. (1994); available from World Data Center-A for Paleoclimatology, National Geophysical Data Center, Boulder, Colorado). Insolation from Berger and Loutre (1991).

from ~9 to 14 (Figure 7). C/N is relatively high (12–14) but variable in sediment older than ~22 ka. The ratios decrease sharply at ~22 ka, just above the top of the clay-rich layer, and attain their lowest and least variable values during the subsequent ~5000 yr interval. C/N fluctuates markedly between 250 and 300 cm, just prior to the Holocene, and are moderately variable during the Holocene, averaging ~11.

The $\delta^{13}C$ of the organic matter ranges from about –30.0 to –25.5‰. Values generally increase from the base of the core to the top of the clay-rich layer, then decrease to their minimum value ~14 ka (280 cm). From this minimum, $\delta^{13}C$ values increase upward by more than 4‰, reaching their highest values at the top of the core.

Diatoms

We analyzed a few sediment intervals (in AL-2) for diatom assemblages to interpret the paleoenvironmental changes associated with the major lithostratigraphic transition associated with the clay-rich interval. One of the two samples from the clay-rich interval (AL-2, 316 cm) had too few diatoms (only four valves were found along three transects of the coverslip) for environmental inferences. The second

Table 3. Principal diatom genera (% relative abundance), Arolik Lake core AL-2.

Depth (cm)	*Achnanthes*	*Aulacoseira*	*Cyclotella*	*Cymbella*	*Navicula*	Small benthic *Fragilaria*	Total plankton
100	11.0	9.8	42.5	2.0	4.6	18.2	55.1
129	2.7	1.4	71.3	3.6	4.8	8.4	72.9
316*	very sparse diatom flora						
340*	12.8	10.1	18.3	4.7	6.4	30.6	28.4
428	11.7	2.0	54.4	1.4	13.8	5.3	57.0
452	11.2	5.1	62.7	1.0	11.7	1.0	67.8

*Sample from clay-rich interval.

sample from the clay-rich interval (AL-2, 340 cm) also contained a low concentration of diatoms, although sufficient to analyze. In addition to the much lower concentration of valves, the most striking difference between the diatom assemblage of the clay-rich sample compared to samples from above and below this interval is its lower proportion of planktonic taxa (Table 3). This reduction in planktonic forms is primarily driven by the decline in *Cyclotella* spp. (mostly *C. tripartita*, *C. rossii*, and *C. comensis*), which are largely replaced by small benthic *Fragilaria* spp. (*F. brevistriata*, *F. pseudoconstruens*, *F. pinnata*).

Discussion

Glacial-lake overflow into Arolik Lake during the last glacial maximum

Our glacial-geologic mapping shows that an ice-marginal lake formed within the unnamed basin adjacent to Arolik Lake as the Goodnews River valley outlet glacier expanded to the G4 moraine (Figure 2A). The ice-dammed lake attained a surface area of ~2 km^2 before reaching its threshold at ~156 m asl (~500 ft) and spilling northwestward into Arolik Lake. Evidence for the former ice-dammed lake includes: (1) rhythmically laminated, inorganic mud exposed in a river bank at the bottom of the unknown tributary valley; (2) a large kame delta bordering the G4 moraine at ~156 m asl; (3) a series of wave-cut shoreline scarps that rim the valley walls up to ~156 m; and (4) an overflow notch at the basin threshold, also at ~156 m. In addition, the overflow from the ice-dammed lake is recorded as an abrupt change in the sediment within Arolik Lake.

We interpret the interval of clay-rich sediment to represent the overflow of this ice-dammed lake during the LGM, and the granules and pebble to record ice-rafted detritus. The clay-dominated grain size probably resulted from the settling of silt-sized particles in the ice-dammed lake prior to spillover into Arolik Lake. The interpretation of this unit is supported by the almost complete absence of diatoms in one of the samples from this interval, and a reduction in planktonic species in the other (Table 3). Restricted ice-free conditions, which have been used to explain the dominance of benthic diatoms as well as sparse diatom floras in deep high-arctic lakes (reviewed in Douglas and Smol (1999)), may be responsible for the strong shifts in the Arolik Lake diatom assemblage. The sparse and benthic-dominated diatom assemblage might also have been promoted by decreased light availability and increased sedimentation rates. These are consistent with the high clay content of the sediment, which probably records a turbid water column. Such an environment would reduce the competitiveness of planktonic diatoms, as they would have to remain buoyant in a more restricted photic zone. The relatively high abundance of the small benthic *Fragilaria* in the Holocene sample (i.e. 100 cm) is difficult to explain at present. Regardless, changes in the diatom flora support the suggestion that glacier meltwater entered Arolik Lake during the deposition of the clay-rich sediment. BSi content is lower in the clay-rich interval than anywhere in AL-4, consistent with the sparse diatom counts in indicating low aquatic productivity, or perhaps dilution by rapid clay deposition, or both. The low OM content with relatively high C/N suggests that, of the little organic matter that was deposited during the period of glacial inflow, much of it was derived from terrestrial rather than aquatic sources.

The ^{14}C age of the clay-rich unit closely dates the maximum ice extent in the Goodnews River valley. The age of the base of this interval is well constrained by a ^{14}C age of ~24 ka at 693–691 cm, 10 cm be-

low the interval. The closest ^{14}C age to the top of the clay is 95 cm above it, at 481 cm (Figure 5). Extrapolating the second-order polynomial fit to the top of the clay-rich interval yields an age of ~22 ka. Thus the outlet glacier in the Goodnews River valley reached its LGM limit ~24 ka; the glacier stabilized long enough to construct the prominent G4 moraine, then retreated ~22 ka when meltwater overflow ceased.

This age can be compared with a previously published ^{36}Cl age on a moraine formed by another outlet glacier of the Ahklun Mountain ice cap located ~45 km to the northeast and traceable to the Goodnews River valley moraine (Figure 1; Briner and Kaufman (2000)). The ^{36}Cl age of 19.6±1.4 ka (n=4 boulder samples) (Briner et al. 2001) overlaps at ±2σ with the ^{14}C-modeled age at the top of the clay-rich interval in AL-4, which marks the cessation of meltwater overflow. If the surface-exposure age is younger, it might indicate a lag between deglaciation and moraine stabilization, or abandonment of the ice-dammed-lake overflow prior to complete retreat of ice from the G4 moraine. Alternatively, the Cl production rates used to calculate the exposure ages might be slightly high. Regardless, once the glacier retreated, it restabilized ~20 km upvalley where it deposited the G3 moraine (Figure 1). The age of this moraine is constrained by a close minimum-limiting ^{14}C age of 19,950±250 yr (Manley et al. 2001).

Glaciers around the globe reached their maximum extent sometime around 25–15 ka, but the age of the LGM varies from place to place. Only in a few places is the age of the local LGM known within narrow limits, especially in Alaska (Hamilton 1994). Differences in the timing of the local LGM reflect the modulation of large-scale forcing by regional-scale features of the climate system. In the Goodnews River valley, the principal outlet glacier emanating from the Ahklun Mountain ice cap expanded to its LGM limit as summer insolation at this latitude reached its minimum; it retreated as insolation increased slightly (Figure 7). The synchroneity between summer insolation and ice extent suggests that the mass balance of the outlet glacier responded sensitively to summer temperature, or to other changes in the climate system related to insolation forcing. For example, anticyclonic circulation over the Laurentide ice sheet may have driven southeasterly moisture into eastern Beringia during the full glacial (Bartlein et al. 1998), providing the additional moisture for the outlet glacier in the Goodnews River valley to attain its LGM position. On the other hand, BSi and OM in AL-4 show that paleoproductivity declined to its lowest levels as the glacier reached its LGM position, indicating that temperature reduction, not moisture increase, drove the positive glacier mass balance that lead to the LGM expansion. In contrast, the readvance of local (cirque-sourced) alpine glaciers 18–16 ka indicates that moisture availability rather than temperature reduction drove subsequent, short-lived positive mass-balance changes in the southwestern Ahklun Mountains (Briner and Kaufman 2000).

Long-term trends in the sediment record

Variations in our multi-proxy records in four cores from Arolik Lake show consistent overall trends that reflect major paleoenvironmental changes. OM and BSi in sediments from other lakes studied previously in southwestern Alaska fluctuated in concert with global climatic changes and appear to respond to climatic variations interpreted based on pollen data (Hu et al. 2002). In Arolik Lake sediment, these indices of productivity show important similarities and differences compared with other records of paleoclimatic change, including oxygen isotopes in Greenland ice (GISP2; Meese et al. (1994)), and with insolation forcing (Berger and Loutre 1991) (Figure 7).

We focus this discussion on core AL-4, where the sedimentation rate is relatively high and the geochronology most reliable, and subdivide the record into four broad intervals (Figure 7): (1) late interstadial (~33–30 ka; 860–770 cm); (2) full glacial (~30–15 ka; 770–330 cm); (3) transitional (~15–11 ka; 330–220 cm); and (4) interglacial (=Holocene; 11–2 ka; 220–0 cm).

Late interstadial

During the first half of the late interstadial interval, which correlates with the end of the middle Wisconsin interstadial (marine oxygen-isotope stage 3), OM and BSi content reach peaks similar to those of the transitional interval that followed the LGM. These proxies record relatively high aquatic productivity, as indicated by the high BSi content (up to 25%) with fluctuations that largely parallel those of OM. In addition, δ^{13}C values are relatively depleted through this interval, and the C/N ratios are moderate (except for two samples), suggesting an aquatic source, or mixed aquatic and terrestrial sources (cf. Naidu et al. (2000) and Anderson et al. (2001)). Overall, these

measures of aquatic productivity decrease through the late interstadial interval, consistent with declining summer insolation at this latitude. Superposed on the overall decrease are three prominent peaks in BSi. Although two of the peaks are represented by only one sample, their rapidity and frequency are reminiscent of Dansgaard–Oesschger (D–O) events recorded in Greenland (Dansgaard et al. 1993) and inferred from other terrestrial (Grimm et al. 1993), marine (Behl and Kennett 1996), and lacustrine (Prokopenko et al. 2001) records. The geochronology and sample resolution are not accurate enough, however, to relate specific peaks in BSi and OM to specific D–O events, nor to other rapid paleoenvironmental changes documented during the middle Wisconsin elsewhere in Beringia (recently reviewed by Anderson and Lozhkin (2001)).

The lower section of AL-4 captured only a brief interval of the last interstadial and probably did not extend to the thermal maximum of the middle Wisconsin. Nonetheless, indications of relative warmth late during the middle Wisconsin at Arolik Lake are consistent with other paleoenvironmental records in eastern Beringia (the Boutellier Interval of Hopkins (1982)). For example, peat and organic silt of the upper unit of the Etolin complex (middle Wisconsin) exposed in coastal bluffs of the Nushagak lowland, 130 km southeast of Arolik Lake, indicate that conditions were cooler than modern (Lea et al. 1991), but warmer and more mesic than those of the of the full glacial interval. This is consistent with the OM and BSi values from 33 to 30 ka in AL-4, which are considerably higher than during the subsequent glacial interval, but overall are about 30% lower than Holocene values.

Full glacial

The glacial interval is marked by the lowest OM (<4%) and BSi (<10%) values. This interval includes the clay-rich unit deposited by the spillover of the glacial-dammed lake during the local LGM. Relatively high C/N and $\delta^{13}C$ values suggest an increased proportion of organic matter from terrestrial sources during the deposition of the overflow mud. Following the cessation of meltwater input, C/N decreases, suggesting an increase in aquatic-derived organic matter. Above the clay-rich unit, grain size generally coarsens, with less clay and fine silt, and more sand and coarse silt. This coarsening might reflect increased input of eolian material, consistent with other evidence for increased aridity, windiness, and active sandar area in Beringia (Hopkins 1982), and locally in the Goodnews River valley. The sediment is still finer, however, than in overlying units, suggesting that far-travelled dust might be an important component of clastic material during the last glacial interval. As temperature warmed following the LGM, the active layer deepened, possibly increasing the flux of solifluction-delivered, coarse sediment to the lake shores; although overall sedimentation rate did not increase.

The proxy environmental indicators are more uniform during the full glacial interval than over any other section of the core. OM and BSi decrease in parallel with the decline in summer insolation during this interval. The low productivity at Arolik Lake is consistent with the low temperature represented by $\delta^{18}O$ of Greenland ice, but no major shifts that might be correlated with Heinrich events 1, 2, or 3 are exhibited in Arolik Lake sediment.

Pleistocene–Holocene transition

The transitional interval is characterized by overall increases in OM and BSi; both constituents approximately double over this $\sim$4000 yr period. The transition is not smooth, but is marked by abrupt (centennial-scale) fluctuations. These changes are not the result of dilution by tephra; of the two prominent tephras in this interval, only tephra D (15.1 ka) was sampled, and only for OM (Figure 7). The prominent peaks in OM and BSi between $\sim$14 and 13 ka are associated with dramatic decreases in C/N and $\delta^{13}C$, suggesting an increase in the proportion of aquatically derived organic matter. OM and BSi then decrease abruptly between 13 and 12 ka, and C/N and $\delta^{13}C$ increase, signaling a decline in aquatic productivity. By 11 ka, OM and BSi reach values on par with their Holocene averages. Our low-resolution sampling indicates generally synchronous changes in measures of productivity in Arolik Lake sediment with $\delta^{18}O$ in Greenland ice. Arolik Lake appears to have responded quickly and sensitively to climatically driven changes during the Pleistocene–Holocene transition; similar responses have been document elsewhere in Alaska (e.g., Mann et al. (2001) and Hu et al. (2002)) and globally. Assessing the extent to which the paleoenvironmental changes archived in Arolik Lake lead or lag other proxy climate records awaits the results of more detailed analyses across this interval. The presence of a tephra layer (tephra C), which was depos-

ited early during the Younger Dryas (12.4 ka), should serve as an important stratigraphic marker, at least regionally.

Holocene

Sediment deposited during the present interglacial (Holocene) interval is characterized by overall high OM (average=8%) and BSi (23%) contents, generally twice that of the preceding glacial interval. OM and BSi fluctuate considerably. C/N ratios fluctuate between 10 and 12, with no trend, suggesting a mixture of terrestrial and aquatic OM. The steady increase in $\delta^{13}C$ during this interval, suggests a progressive change in carbon cycling in the system, or an increase in lake productivity (Brenner 1999). Sediments coarsen and exhibit less-distinct layering. These observations are consistent with an increase in the input of solifluction-driven colluvium from adjacent hillslopes as the depth and duration of summer thaw increased, and as permafrost became discontinuous during the Holocene. Aquatic productivity would have intensified in response to increased input of nutrients associated with increased temperature and expended vegetation cover (e.g., Horiuchi et al. (2000)).

The Holocene interval also includes by far the thickest tephra layer that fell at Arolik Lake during the past 33,000 yr (and longer, based on the lower part of AL-2). As expected, OM and BSi reach their minima in the tephra. The tephra fall does not appear to have had a long-lasting impact on the aquatic productivity, as OM and BSi recover to their pre-eruption values immediately above the tephra (note the interruption in the $\delta^{13}C$ and C/N trends, however)

The rapid and dramatic changes in OM and especially BSi in Arolik Lake sediment during the Holocene contrast markedly with the oxygen-isotope record from Greenland ice, which shows relatively little variability during the Holocene compared to the Pleistocene. The high variability in Arolik Lake sediment indicates considerable fluctuations in organic productivity, or perhaps inorganic sediment input, similar to that of the interstadial and transitional intervals. Our chronology and sample resolution are presently inadequate to address whether some of this variability corresponds to Holocene climatic changes documented elsewhere in the Arctic (e.g., Bond et al. (2001)).

Conclusion

The ~33,000 yr record from Arolik Lake affords a long-term perspective on paleoenvironmental change in southwestern Alaska. It is one of a few such records in northwestern North America that span from the end of the last interstadial to the present. The stability of paleoproductivity indicators (especially OM and BSi) during the glacial period (~30–15 ka) suggests that, either these indicators remained insensitive, despite climatic change during this interval, or that few environmental changes took place. Climate did change during this interval, however: the sedimentological data show a dramatic shift as the Goodnews River valley filled with ice from the ice-cap outlet glacier, which dammed an ice-marginal lake that overflowed into Arolik Lake. This overflow, and the maximum extent of glacier ice that it records, took place in step with the summer insolation minimum at 60° N latitude, indicating that glaciers in southwestern Alaska responded to large-scale forcing. A (re)advance of local alpine glaciers between 18 and 16 ka (Briner and Kaufman 2000; Briner et al. 2001) and the series of end moraines in the Goodnews River valley (upvalley from the G4 moraine) shows that climate continued to fluctuate in this region, although the amount of OM and BSi in Arolik Lake sediment did not.

In contrast to the glacial interval, the preceding interstadial and the subsequent Holocene periods exhibit much greater variability, either because environmental changes were more frequent and dramatic, or because the proxy indicators were more sensitive to change during these intervals. We speculate that the flux of water, sediment, and dissolved constituents increased as the active layer deepened, and as runoff and subsurface flow increased under warmer conditions. Superposed on the overall increased aquatic productivity, the lacustrine system seems to have responded more sensitively to climatically driven paleoenvironmental change during the interstadial and the Holocene. The rapid and dramatic fluctuations in OM and BSi throughout the Holocene, and the relatively minor changes during the glacial interval, contrasts markedly with paleoclimatic records from downstream of the Laurentide ice sheet that exhibit the opposite pattern.

Acknowledgements

The Dillingham office of the Togiak National Wildlife Refuge provided critical logistical support; Y. Axford, A. Feinberg, L. Levy, and M. Robinson assisted in the field; W. Manley offered valuable input; S. McMillan and S. Yoneji analyzed the BSi, J. Smol and M. Douglas contributed to the diatom analyses; G. Seltzer loaned us the seismic equipment; J. Turnbull generated the targets for most of the ^{14}C AMS analyses; P. Hallman prepared the pollen concentrates for ^{14}C analysis; two anonymous reviewers suggested improvements; the National Science Foundation (ATM-9808593; EAR-9809330; ATM-0097127) funded this research; this is PARCS contribution #198.

References

Abbott M.B. and Stafford T.W. 1996. Radiocarbon geochemistry of modern and ancient Arctic lake systems, Baffin Island, Canada. Quat. Res. 45: 300–311.

Anderson P.M. and Brubaker L.B. 1994. Vegetation history of northcentral Alaska – A mapped summary of late Quaternary pollen data. Quat. Sci. Rev. 13: 71–92.

Anderson P.M. and Lozhkin A.V. 2001. The Stage 3 interstadial complex (Karginskii/middle Wisconsinan interval) of Beringia: variations in paleoenvironments and implications for paleoclimatic interpretations. Quat. Sci. Rev. 20: 93–125.

Anderson L., Abbott M.B. and Finney B.P. 2001. Holocene paleoclimate from oxygen isotope ratios in lake sediments, central Brooks Range, Alaska. Quat. Res. 55: 313–321.

Bartlein P.J., Anderson K.H., Anderson P.M., Edwards M.E., Mock C.J., Thompson R.S. et al. 1998. Paleoclimate simulations for North America over the past 21,000 years: Features of the simulated climate and comparisons with the paleoenvironmental data. Quat. Sci. Rev. 17: 549–585.

Battarbee R.W., Carvalho L., Jones V.J., Flower R.J., Cameron N.G., Bennion H. et al. 2001. Diatoms. In: Smol J.P Birks H.J.B. and Last W.M. (eds), Tracking Environmental Change Using Lake Sediments. Vol. 3: Terrestrial, Algal and Siliceous Indicators. Kluwer Academic Publishers, Dordrecht, The Netherlands, pp. 55–202.

Behl R.J. and Kennett J.P. 1996. Brief interstadial events in the Santa Barbara basin, NE Pacific, during the past 60 kyr. Nature 379: 243–246.

Berger A. and Loutre M.F. 1991. Insolation values for the climate of the last 10 million of years. Quat. Sci. Rev. 10: 297–317.

Brenner M. 1999. Stable isotope (^{13}C and ^{15}N) signatures of sedimented organic matter as indicators of historic lake trophic state. J. Paleolim. 22: 205–221.

Bond C., Kromer B., Beer J., Muscheler R., Evans M., Showers W. et al. 2001. Persistent solar influence on North Atlantic climate during the Holocene. Science 294: 2130–2136.

Briner J.P. 1998. Late Pleistocene glacial chronology of the western Ahklun Mountains, southwestern Alaska. MSc thesis. Utah State University, 106 pp.

Briner J.P. and Kaufman D.S. 2000. Late Pleistocene glaciation of the southwestern Ahklun Mountains, Alaska. Quat. Res. 53: 13–22.

Briner J.P., Swanson T.W. and Caffee M. 2001. Cosmogenic ^{36}Cl glacial chronology of the southwestern Ahklun Mountains, Alaska: Extensive early Wisconsin ice. Quat. Res. 56: 148–154.

Colman S.M., Peck J.A., Karabanov E.B., Carter S.J., King J.W. and Williams D.F. 1995. Continental climate response to orbital forcing – The diatom paleoproductivity record from Lake Baikal, Siberia. Nature 378: 769–771.

Dansgaard W., Johnsen S.J., Clausen H.B., Dahl-Jensen D., Gundestrup N.S., Hammer C.U. et al. 1993. Evidence for general instability of past climate from a 250-kyr ice-core record. Nature 364: 218–220.

Douglas M.S.V. and Smol J.P. 1999. Freshwater diatoms as indicators of environmental change in the high Arctic. In: Stoermer E.F. and Smol J.P. (eds), The Diatoms: Applications for the Environmental and Earth Sciences. Cambridge University Press, Cambridge, pp. 227–244.

Engstrom D.R. and Wright H.E. 1984. Chemical stratigraphy of lake sediments as a record of environmental change. In: Haworth E.Y. and Lund J.W.G. (eds), Lake Sediments and Environmental History. University Press, Leicester, pp. 11–67.

Faegri K., Kaland P.E. and Kryzywinski K. 1992. Textbook of Pollen Analysis. Hafner, New York, 328 pp.

Grimm E.C., Jacobson G.L., Watts W.A., Hansen B.C.S. and Maasch K.A. 1993. A 50,000-yr record of climate oscillations from Florida and its temporal correlation with Heinrich events. Science 261: 198–200.

Hamilton T.D. 1994. Late Cenozoic glaciation of Alaska. In: Plafker G. and Berg H.C. (eds), The Geology of Alaska. Geological Society of America, Boulder, CO, pp. 813–844.

Hoare J.M. and Coonrad W.L. 1961. Geologic map of the Goodnews Quadrangle, Alaska. U.S. Geological Survey Miscellaneous Geologic Investigations Map I-339.

Hopkins D.M. 1982. Aspects of the paleogeography of Beringia during the late Pleistocene. In: Hopkins D.M., Matthews J.V., Jr Schweger C.E. and Young S.B. (eds), Paleoecology of Beringia. Academic Press, New York, pp. 3–28.

Horiuchi K., Minoura K., Hoshino K., Oda T., Nakamura T. and Kawai T. 2000. Paleoenvironmental history of Lake Baikal during the last 23000 years. Palaeogeography, Palaeoclimatology, Palaeoecology 157: 95–108.

Hu F.S., Lee B.Y., Kaufman D.S., Yoneji S., Nelson D. and Henne P. 2002. Response of tundra ecosystem in southwestern Alaska to Younger-Dryas climatic oscillation. Global Change Bio. 8: 1156–1163.

Hu F.S., Brubaker L.B. and Anderson P.M. 1995. Postglacial vegetation and climate change in the northern Bristol Bay region, southwestern Alaska. Quat. Res. 43: 382–392.

Kitagawa H. and van der Plicht J. 1998. Atmospheric radiocarbon calibration to 45,000 year B.P., late glacial fluctuations and cosmogenic isotope production. Science 279: 1187–1190.

Kutzbach J., Coe M. and Foley J. 1997. Testing the accuracy of arctic system model of simulation of century-to-millennia-scale variability: Modeling the arctic system – A workshop report on

the state of modeling in the Arctic System Science Program. The Arctic Research Consortium of the United States, Fairbanks, Alaska, pp. 58–59.

Lea P.D., Elias S.A. and Short S.K. 1991. Stratigraphy and paleoenvironments of Pleistocene nonglacial deposits in the southern Nushagak lowland, southwestern Alaska, U.S.A. Arctic and Alpine Res. 23: 375–391.

Manley W.F., Kaufman D.S. and Briner J.P. 2001. Late Quaternary glacier fluctuations in the southern Ahklun Mountains, southeast Beringia, soil development, morphometric, and radiocarbon constraints. Quat. Sci. Rev. 20: 353–370.

Mann D.H., Peteet D.M., Reanier R.E. and Kunz M.L. 2001. Responses of an arctic landscape to late glacial and early Holocene climatic changes, the importance of moisture. Quat. Sci. Rev. 21: 997–1021.

Meese D.A., Alley R.B., Fiacco R.J., Germani M.S., Gow A.J., Grootes P.M. et al. 1994. Preliminary depth-age scale of the GISP2 ice core. Special CRREL Report 94-1.

Meyers P.A. and Ishiwatari R. 1993. The early diagenesis of organic matter in lacustrine sediments. In: Engels M.H. and Macko S.A. (eds), Organic Geochemistry – Principles and Applications. Plenum Press, New York, pp. 185–209.

Miller G.H., Mode W.N., Wolfe A.P., Sauer P.E., Bennike O., Forman S.L. et al. 1999. Stratified interglacial lacustrine sediments from Baffin Island, Arctic Canada, chronology and paleoenvironmental implications. Quat. Sci. Rev. 18: 789–810.

Mortlock R.A. and Froelich P.N. 1989. A simple method for the rapid determination of biogenic opal in pelagic marine sediments. Deep-Sea Res. 36: 1415–1426.

Naidu A.S., Cooper L.W., Finney B.P., Macdonald R.W., Alexander C. and Semitelov I.P. 2000. Organic carbon isotope ratios ($\delta^{13}C$) of Arctic Amerasian continental shelf sediments. Int. J. Earth Sci. 89: 522–532.

Oswald W.W., Anderson P.M., Brown T.A., Brubaker L.B., Hu F.S., Lozhkin A.V. and Tinner W. 2002. Effects of sample mass and type on ^{14}C dating of Beringian lake sediments. NSF-ARCSS All-Hands Workshop, 22–22 February. The Arctic Research Consortium of the United States, Fairbanks, Alaska, p. 125.

Overpeck J., Hughen K., Hardy D., Bradley R., Case R., Douglas M. et al. 1997. Arctic environmental change of the last four centuries. Science 278: 1251–1256.

Péwé T.L. 1975. The Quaternary Geology of Alaska. U.S. Geological Survey Professional Paper 385: 145 pp.

Prokopenko A.A., Williams D.F., Karabonov E.B. and Khursevich G.K. 2001. Continental response to Heinrich events and Bond cycles in sedimentary records of Lake Baikal, Siberia. Global and Planetary Change 28: 217–226.

Stuiver M., Reimer P.J., Bard E., Beck J.W., Burr G.S., Hughen K.A. et al. 1998. INTCAL98 Radiocarbon age calibration, 24,000–0 cal BP. Radiocarbon 40: 1041–1083.

Thompson R. and Oldfield F. 1986. Environmental Magnetism. Allen and Unwin, London, 227 pp.

Waythomas C.F. and Neal C.A. 1998. Tsunami generation by pyroclastic flow during the 3500-year B.P. caldera-forming eruption of Aniakchak Volcano, Alaska. Bul. Volcanol. 60: 110–124.

Wetzel R.G. 1983. Limnology. Saunders College Publishing, New York, 858 pp.